

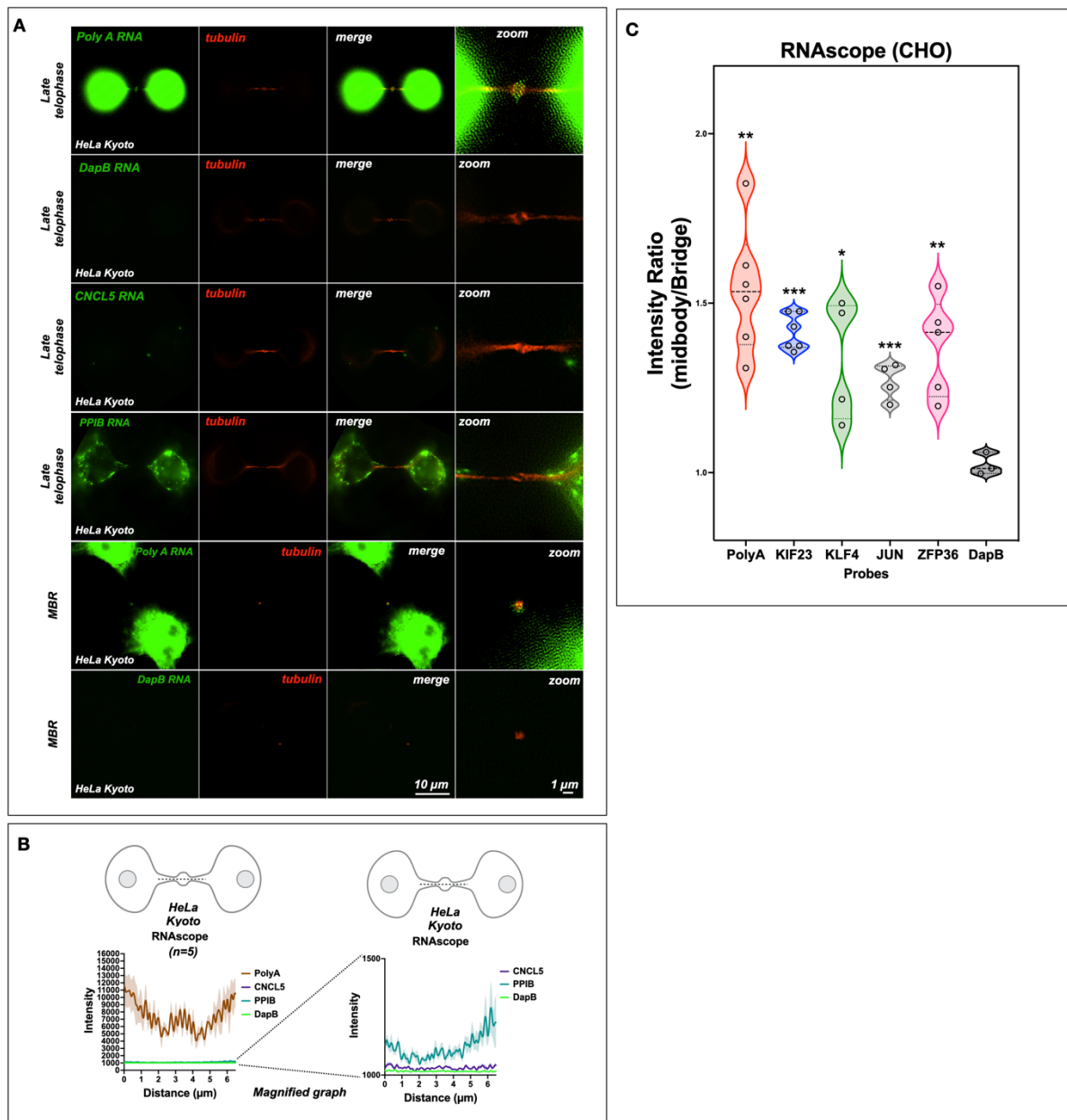
**Figure S1: The midbody proteome revealed 99 RNA-binding proteins and factors that are specifically found during late telophase/G1 and in MBRs, related to STAR Methods.**

(A) Previously identified Midbody RBPs localize to MB during G1 and are packaged into the MBR. We observed puncta along the microtubules as well as in the MB dark zone. Stau, however, is found primarily along the bridge, in a faint ring where we also see ribosomes, and is found in the MBR.

(B) MB proteome analyses re-sorted just for RNA binding proteins from in the Supplemental data tables in Skop et al., 2004, identified 99 RNA-binding proteins. When binned by gene ontology terms, many functions in addition to RNA-binding were identified, including DNA binding, cell division, growth, proliferation, development, differentiation, and apoptosis.

(C) Of the 22 MB-enriched mRNAs in Fig. 1C, most (n=10/12 assayed) encode proteins that were undetectable until the G1 transition. These include many transcription factors with no known role in cytokinesis, in an environment lacking DNA, suggesting a role in post-mitotic function. MKLP1 and TEX14 have known roles in cytokinesis and were present throughout the MB stages.

Scale bars are 1  $\mu$ m unless noted.



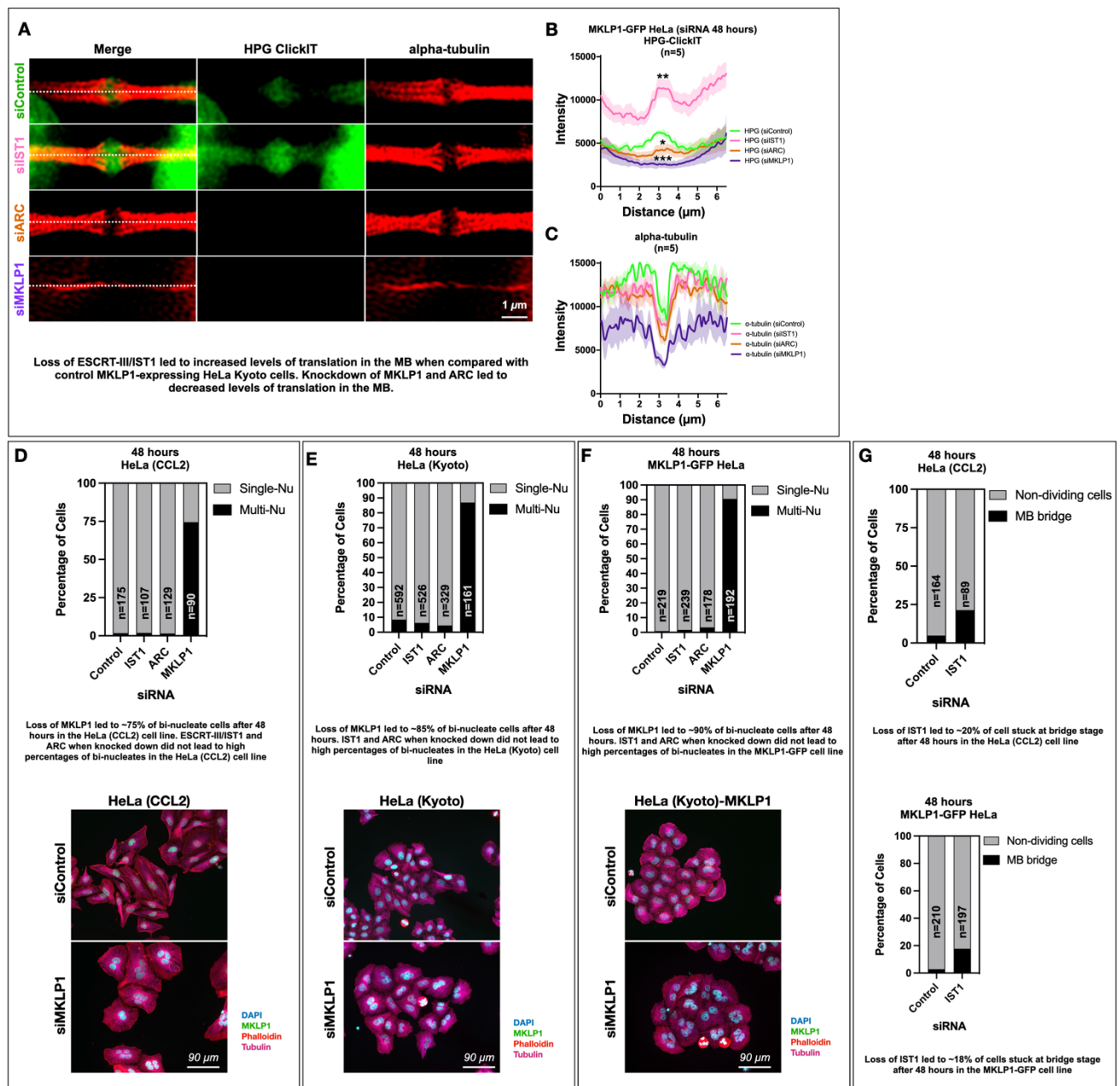
**Supplemental Figure S2: Poly A localization in whole cells and at the midbody in HeLa Kyoto cells, related to Figure 1.**

**(A)** Poly A signal is detected in whole cell bodies and at the midbody (Zoom). DapB, a bacterial RNA, does not localize to the cell body or midbody during late Telophase. CNCL5 and PPIB, identified in our midbody RNA seq data as being in a group of the least enriched RNAs, were not found in the midbody (CNCL5 & PPIB), but PPIB was found in the cell body. PolyA was found in the cell body and MBR and DapB was not found in MBRs.

**(B).** Quantification of PolyA, CNCL5, PPIB and DapB in the midbody in HeLa Kyoto cells. Here, PolyA is highly enriched whereas the other control RNAs are not. A magnified graph shows a detailed view of the intensity at the midbody for CNCL5, PPIB and DapB.

**(C).** Quantification of RNAscope probe intensities for PolyA, KIF23, KLF4, JUN and ZFP36 in CHO cells compared to DapB (control RNAscope probe) (refer to Fig 1J for images). Here, PolyA is highly enriched, whereas KIF23, KLF4, JUN and ZFP36 are less so. DapB (control) is not enriched. Asterix denotes significance.

Scale bars are 1  $\mu$ m unless noted.



**Supplemental Figure S3: Comparison of siRNA knockdown in HeLa (CCL2) cells and in HeLa cells overexpressing MKLP1-GFP, related to Figure 2.**

(A-C) Loss of ESCRT-III/IST1 led to increased levels of translation in the MB dark zone and decreased levels of translation when *MKLP1* and *ARC* were knocked down in the MKLP1-GFP-overexpressing HeLa cell line. Statistical significance is denoted with an Asterix.

(D-F) Loss of MKLP1 after *MKLP1* siRNA treatment led to 75% binucleate cells in the HeLa (CCL2) cell line (D), and 85% binucleate cells in the HeLa Kyoto cell line (E), and 90% in the MKLP1-GFP-overexpressing HeLa Kyoto cell line (F). *ESCRT-III/IST1* and *ARC* siRNA did not lead to high levels of binucleate cells in either the HeLa (CCL2) cells (D), HeLa Kyoto (E), or the MKLP1-GFP-overexpressing HeLa Kyoto cell line (F).

(G) Loss of ESCRT-III/IST1 led to approximately 20% to be stuck at bridge stage after 48 hours in the HeLa (CCL2) cell line (top) and approximately 18% of cells in the MKLP1-GFP-overexpressing HeLa Kyoto cell line (bottom)

Con: control.

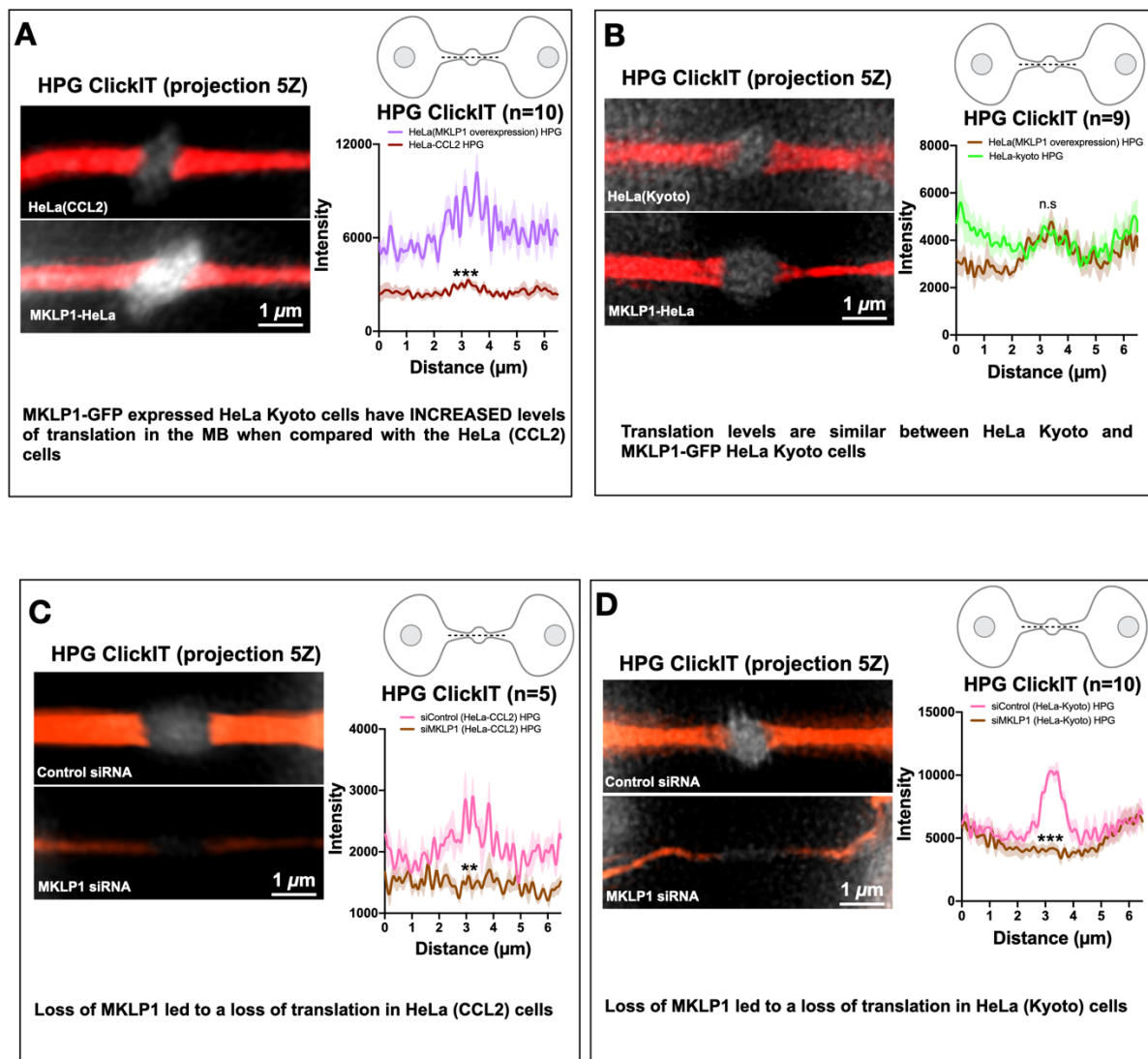


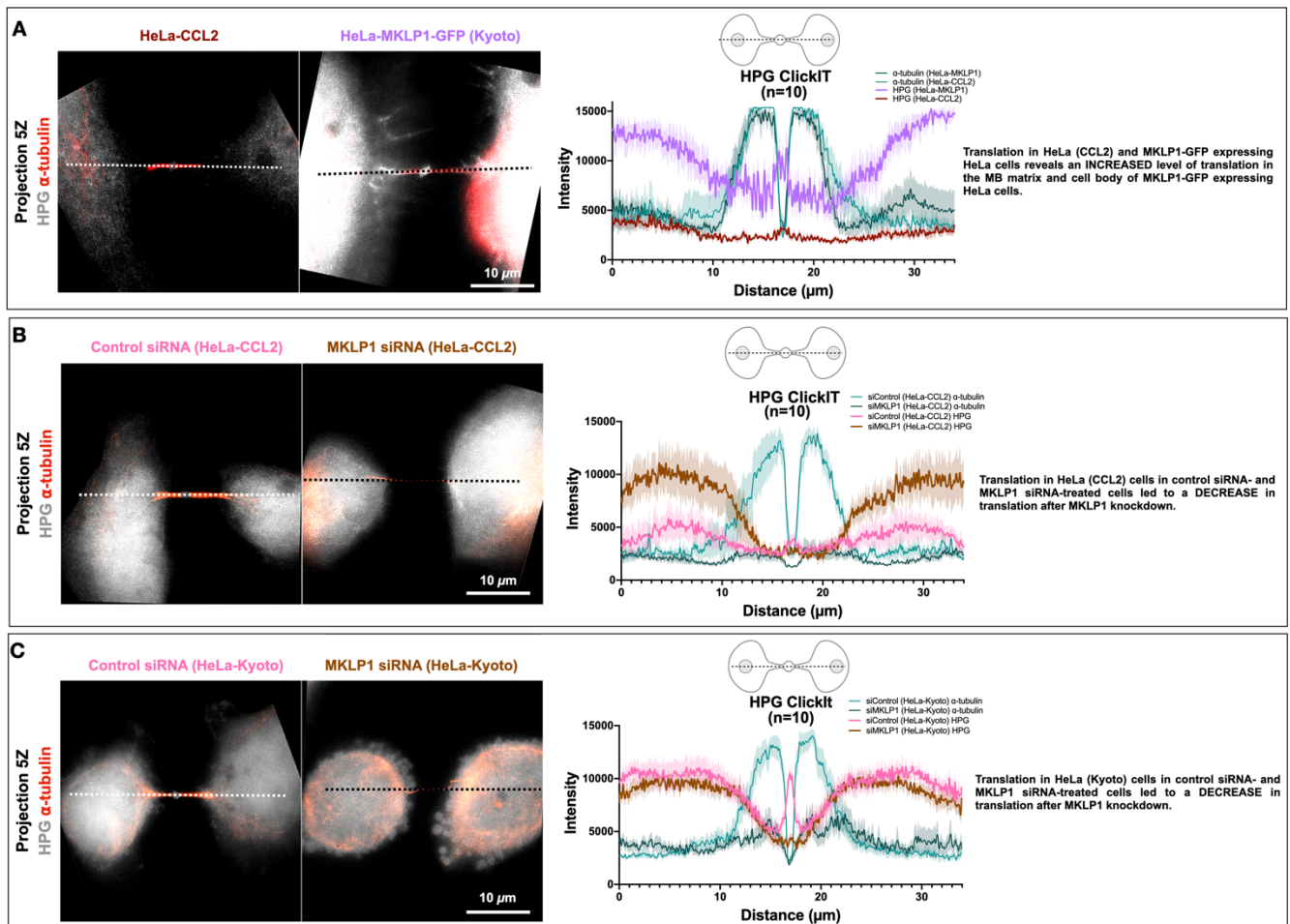
**Figure S4: Active translation is different between HeLa CCL2 and HeLa Kyoto cell lines and is mediated by MKLP1, related to Figure 5.**

**(A)** A remarkable increase in translation was observed in MKLP1-GFP-overexpressing HeLa Kyoto cells compared with HeLa (CCL2) cells, as visualized by HPG-ClickIT signals. This suggests that MKLP1 itself may regulate levels of translation in general. Significance is noted by an asterix.

**(B)** Comparison of the HPG-ClickIT signal in the dark zone of the MB using line scans of the intercellular bridges between HeLa (Kyoto) and MKLP1-GFP HeLa (Kyoto). No differences in translation were observed between HeLa Kyoto and the MKLP1-GFP HeLa Kyoto cell line however.

**(C)** Quantification of the HPG-ClickIT signal in the dark zone of the MB using line scans of the intercellular bridges. A decrease in translation was observed in HeLa (CCL2) native cell lines after MKLP1 knockdown by siRNA treatment, suggesting that MKLP1 may regulate translation in some way. Significance is noted by an asterix.

**(D).** Quantification of the HPG-ClickIT signal in the dark zone of the MB using line scans of the intercellular bridges. A decrease in translation was observed in HeLa (Kyoto) cell lines after MKLP1 knockdown by siRNA treatment, suggesting that MKLP1 may regulate translation in some way. Significance is noted by an asterix.



**Supplemental Figure S5: Translation levels are regulated by MKLP1, related to Figure 5.**

**(A)** To quantify the translation levels in whole cells, HeLa (CCL2) cells (brown) and MKLP1-GFP-overexpressing HeLa Kyoto cells (purple) were compared. There was a significant increase in HPG-ClickIT signals in both the cell body and MB in the MKLP1-GFP-overexpressing HeLa Kyoto cells, suggesting that MKLP1 likely plays a role in mediation of translation levels in general.

**(B)** Knockdown of MKLP1 (brown) in HeLa CCL2 cell lines leads to a decrease in HPG-ClickIT signal (translation) when compared to controls (pink).

**(C)** Knockdown of MKLP1 in HeLa Kyoto cell lines leads to a decrease in HPG-ClickIT signal (translation). Translation was localized to the cell body and the MB dark zone.

The tubulin scan (teal) is represented in the charts to show where the MB dark zone is located, denoted by the dip in tubulin signal. Here, the increase or decrease in translation can be observed easily.

Quantification is noted above each graph.  
Scale bars are 10 $\mu$ m.